GT-2004-53613

DEVELOPING A COMBUSTOR SIMULATOR FOR INVESTIGATING HIGH PRESSURE TURBINE AERODYNAMICS AND HEAT TRANSFER

M.D. Barringer and K. A. Thole
Mechanical Engineering Department
Virginia Polytechnic Institute and State University
Blacksburg, VA 24061

M.D. Polanka
Air Force Research Laboratory
Turbines Branch
WPAFB, OH 45433

ABSTRACT

Within a gas turbine engine, the high pressure turbine vanes are subjected to very harsh conditions from the highly turbulent and hot gases exiting the combustor. The temperature and pressure fields exiting the combustor dictate the heat transfer and aero losses that occur in the turbine passages. To better understand these effects, the goal of this work is to develop an adjustable combustor exit profile simulator for the Turbine Research Facility (TRF) at the Air Force Research Laboratory (AFRL). The TRF is a high temperature, high pressure, short duration blow-down test facility that is capable of matching several aerodynamic and thermal non-dimensional engine parameters including Reynolds number, Mach number, pressure ratio, corrected mass flow, gas-to-metal temperature ratio, and corrected speed.

The research objective was to design, install, and verify a non-reacting simulator device that provides representative combustor exit total pressure and temperature profiles to the inlet of the TRF turbine test section. This required the upstream section of the facility to be redesigned into multiple concentric annuli that serve the purpose of injecting high momentum dilution jets and low momentum film cooling jets into a central annular chamber, similar to a turbine engine combustor. The design of the simulator allows for variations in injection levels to generate turbulence and pressure profiles. It also can vary the dilution and film cooling temperatures to create a variety of temperature profiles consistent with real combustors. To date, the design and construction of the simulator device has been completed. All of the hardware has been trial fitted and the flow control shutter systems have been successfully installed and tested. Currently, verification testing is being performed to investigate the impact of the generated temperature, pressure, and turbulence profiles on turbine heat transfer and secondary flow development.

NOMENCLATURE

A   flow area or surface area
c_p specific heat
D   hole diameter
G   mass flow velocity, $G = \dot{m}/A_{ff}$
h   convection heat transfer coefficient

I   momentum flux ratio, $I = \left(\rho_{jet} V_{jet}^2\right)\Big/\left(\rho_\infty V_\infty^2\right)$

j   Colburn factor , $j = \left(h_{gas} \cdot Pr^{2/3}\right)\Big/\left(G \cdot c_{p_{gas}}\right)$

L   overall length
P   pressure
PF   pattern factor, $PF = \left(T_{max} - T_{ave}\right)/\Delta T_{combustor}$
Pr   Prandtl number
Re   Reynolds number
RTDF   Radial temperature distortion factor,

$$RTDF = \frac{T - T_{ave}}{T_{ave} - T_{coolant}}$$

S   vane span
t   time
T   temperature
V   velocity
Vol   volume
X,Y,Z   distance in axial, pitch, and span directions

Greek

β   annular flow path solidity, $\beta = 1 - A_{open}/A_{annulus}$

ρ   density

Subscripts

∞   freestream or mainstream
0   total conditions
1   first row dilution holes
2   second row dilution holes
ave   average
FC   film cooling holes
ff   cross-sectional free flow area in heat exchangers
gas   gas flowing through the annulus
i   initial conditions
jet   dilution jet or film cooling jet
metal   heat exchanger metal or rig metal
ms-ave   mid-span average
open   total open flow area.

INTRODUCTION

The recent strive towards increasing the turbine working temperature has put incredible emphasis on understanding just how the combustor exit flow interacts with and affects the

performance of the downstream turbine. The complex temperature and pressure profiles exiting combustors have forced engine designers to prepare for the worst case without knowing exactly how the profiles affect the hardware.

Radial as well as circumferential variations in pressure, temperature, turbulence intensity and scale are produced within the combustion chamber and all combine to yield a very complex exit flow structure. The spatial variations in temperature migrate through the combustion chamber and impose non-uniform heat loading on the downstream high pressure turbine vanes that can result in portions of individual vanes melting and cracking and in some circumstances being destroyed. Variations in turbulence intensity and scale can exacerbate this heat loading by increasing local convection heat transfer coefficients to the vane surface thereby increasing the surface heat flux. The spatial variations in pressure exiting the combustor result in non-uniform aerodynamic loading on the vanes. Turbine designers currently often use a pressure profile consistent with a standard turbulent boundary layer as the inlet condition to the turbine while designing their vanes and blades. The non-uniform combustor exit pressure profiles can result in turbine inlet profiles and secondary flow development that is different than what is currently predicted.

The major features of combustion chambers in aircraft gas turbine engines include the chamber liners, swirlers, fuel nozzles, dilution holes, film cooling holes and slots, and an overall exit contraction. One major design consideration is the division of mass flow into separate flow paths to cool the metal casing and dilute the combustion products. The interaction of the flow streams passing through these combustor components results in a very complex flowfield exiting the combustor and entering the downstream turbine section. Several non-reacting and reacting experimental and computational studies have been performed to analyze and model these combustor flows, however, very few have focused on the effects that this flowfield has on the downstream turbine.

Holdeman [1] conducted experiments and computations on dilution jets by studying the mixing of single, double, and opposed rows of dilution jets in a non-reacting combustor model. The principle finding was that the jet momentum flux ratio dictated the combustor exit velocity and temperature profiles. The opposed rows of jets resulted in the most effective and rapid mixing. Computational models using the standard k-ε turbulence model did not accurately predict the mixing of opposed dilution jet injection, but predicted the jet penetration very well.

High-intensity large-scale turbulence in a non-reacting combustor simulator was studied by Ames and Moffat [2]. Their experimental model contained slot film cooling, two rows of in-line dilution holes, and a 50% exit contraction that generated turbulence intensity levels up to 19% and integral length scales that scaled well with the dilution hole diameters. They reported that heat transfer was augmented by up to 26% for a turbulent boundary layer over a flat plate with constant velocity. Barringer et al. [3] and Stitzel and Thole [4] also tested and computationally modeled a non-reacting combustor simulator containing liners with film cooling holes and two rows of in-line dilution jets that produced similar turbulence intensity levels near 18%. The computational models used the RNG k-ε turbulence model and the results agreed with those found by Holdeman [1] in that turbulence was underpredicted.

Swirl driven inlet flow was studied by Cameron et al. [5] in non-reacting and reacting model combustors with wall injection. They concluded that the strong recirculation zone located upstream of the primary jets present in the non-reacting case was dissipated in the case of reaction. Velocity measurements in the exit plane indicated turbulence levels near 25% for the reaction case, which is consistent with the studies without reaction.

Turbulence was studied in two reacting models by Bicen et al. [6] that included liner cooling slots and two rows of dilution jets. The results indicated non-uniform distributions of velocity in the combustor exit plane and turbulence levels near 20% over the majority of the exit plane. These levels are consistent with the results presented earlier for the non-reacting combustor studies indicating that reactions do not significantly contribute to turbulence levels. The temperature profiles at the combustor exit plane were also found to be non-uniform.

Schwab et al. [7] and Stabe et al. [8] conducted analytical and experimental studies of flow through a turbine stage with uniform and non-uniform inlet radial temperature profiles. The profiles were generated using a Combustor Exit Radial Temperature Simulator (CERTS) by injecting coolant air through circumferential slots in the hub and tip endwalls upstream of the stator vanes. Coolant flow rates were adjusted to produce design inlet temperature profiles in terms of local to mean temperature ratios. Chana et al. [9] also designed and tested a non-uniform inlet temperature generator for a transient turbine research facility. Cold gas was injected upstream of the turbine section at the hub and tip to shape the temperature profile in the radial direction and through turbulence rods inserted into the main flow to shape it in the circumferential direction. Results showed vane heat transfer was affected by the presence of the non-uniform temperature profile only on the vane suction surface.

Krishnamoorthy et al. [10] investigated the effect of combustor turbulence on a downstream turbine vane cascade. Their results indicate that the effect of high turbulence at the combustor exit was to reduce the cooling effectiveness on the vane by 10%. It was also shown that the effect of temperature non-uniformities at the combustor exit was to reduce the overall cooling effectiveness on the vane by as much as 21%

Colban et al [11] studied the effects of varying film cooling flow through the liner and exit junction slot in a large-scale (9X), low speed combustor simulator on the adiabatic effectiveness and secondary flow development within a downstream turbine cascade. Results showed that varying the coolant injection through the liner led to different total pressure profiles entering the downstream turbine section. Measurements showed that the coolant exiting the liner and slot accumulated along the suction side of the vane and endwall and that increasing the film cooling flow through the liner did not result in a continual increase in adiabatic effectiveness values.

The literature indicates that the most significant components that contribute to the non-uniform exit thermal and pressure fields are swirlers, film cooling slots and holes, and dilution holes. The studies also indicate that thermal fields downstream of the primary zone are very similar with or without reaction. The only noteworthy differences occur upstream of the primary zone where combustion is stabilized. This is important because it allows a flow field representative of one exiting a real gas turbine combustor to be simulated

under non-reacting conditions without swirl. There is insufficient research, however, that incorporates the effects of realistic combustor flow and thermal fields on downstream turbine vanes and endwall regions. Very little experimental data exists that documents total pressure profiles at the combustor exit. This information is paramount since it has been shown in Hermanson and Thole [12] and in Colban et al. [11] that the total pressure field is a driving force in the development of secondary flows present in the downstream nozzle guide vane passages. These secondary flows dictate the heat transfer to the endwall regions by lifting cooler fluid near the endwall and replacing it with hotter mainstream fluid.

A better understanding of how the combustor exit flow affects the flow development and heat transfer within the downstream turbine is needed. It is for this reason that a device was designed to simulate the conditions exiting typical engine combustors. The primary research objective was to design, install, and verify a non-reacting simulator device that can provide representative combustor exit pressure and temperature profiles with realistic turbulence levels to the inlet of a true scale, fully annular, high pressure turbine rig that is located in the TRF at AFRL. The approach of this research was to first analyze several representative temperature and pressure profiles exiting actual aircraft engine combustors. These profiles were used to design a structure that could be installed upstream of the main turbine test section in the TRF. Once the simulator is installed several benchmarking experiments will be conducted to verify its performance. The affects of adjusting the combustor exit profiles of pressure, temperature, and turbulence on turbine vane heat flux and secondary flow development will be studied. The focus of this paper is to present the overall design of the simulator.

COMBUSTOR SIMULATOR REQUIREMENTS

To design a simulator device that can produce representative combustor exit conditions it was necessary to contact engine manufacturers and researchers. Several different radial and some circumferential profiles of temperature and pressure were obtained from the General Electric Company, Pratt & Whitney Engines, and the Air Force Research Laboratory. This data in conjunction with several combustor simulator exit pressure profiles documented in Colban et al. [11] was studied to help determine the proper radial profile shapes that the simulator should be capable of producing.

The pressure profiles, shown in non-dimensional form in Figure 1, exhibit relatively constant pressure in the near mid span region while some display a pronounced peak in the near endwall region. The mid span behavior can be explained by the significant amount of dilution present in the combustor that results in very thorough mixing of the flow. The behavior seen in the near endwall region can be attributed to varying amounts of upstream film cooling flow that passes through the combustor liner. Some of the radial temperature profiles that were obtained are shown in Figure 2. These temperature profiles are also displayed in non-dimensional form. Most of these temperature profiles exhibit a peak in the mid-span region corresponding to the upstream fuel nozzles in the combustor. The radial locations of minimum temperature may be at the hub for some engines and it may be at the tip for other engines. The

capability to simulate these types of profiles will be the primary motivator behind the design of the combustor simulator.
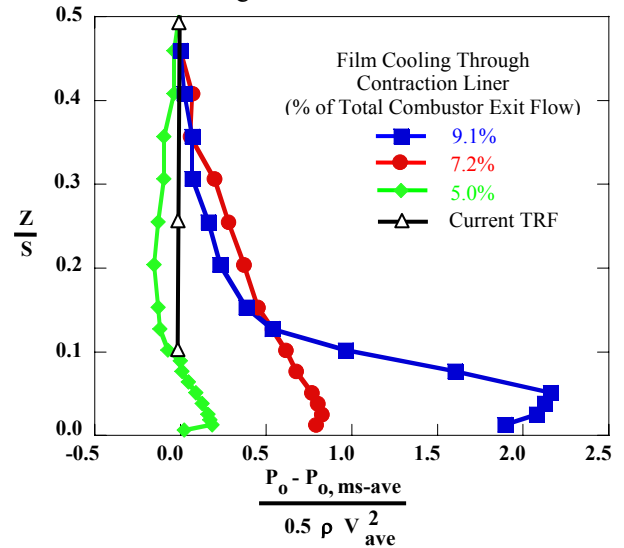

Figure 1. Spanwise total pressure profiles at the combustor simulator exit from Barringer et al. [3] and Colban et al. [11] compared with the present TRF.
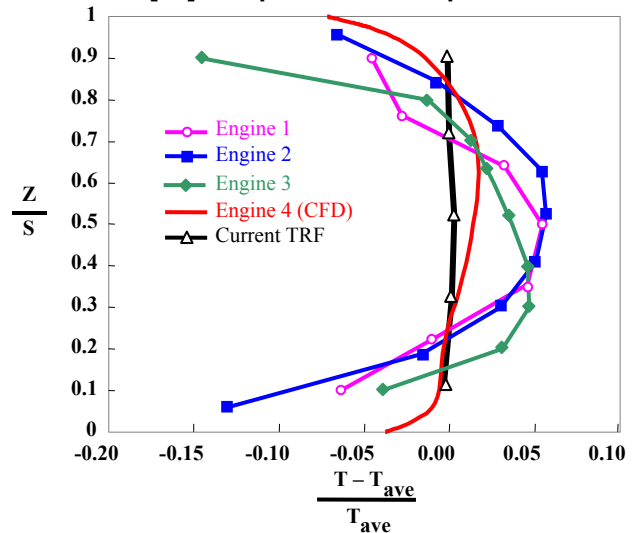

Figure 2. Radial temperature profiles at the exit of the combustor from several engine manufacturers.

It is worth noting that the combustor exit temperature profile can be arranged in several non-dimensional forms. Engine manufacturers typically use the pattern factor, PF, to document the performance of their combustors. This pattern factor definition, however, only applies to actual combustors as it references the temperature rise across the combustor. In a simulator, the inlet condition is irrelevant and only the profiles entering the turbine are of interest. The non-dimensional form shown in Figure 2 was chosen for comparing the engine temperature profiles with those produced by the simulator device. This is in contrast to the non-dimensional form presented in Chana et al. [9] where a radial temperature distortion factor, RTDF, was defined. A nearly constant radial temperature profile where the mean temperature is relatively close to both the maximum and minimum temperatures

possesses significant shape when plotted in the RTDF form. This is illustrated in Figure 3 where the current TRF turbine inlet profile in Figure 2 has been re-plotted into the RTDF form, along with the same engine profiles. In Figure 3, the coolant temperature used for the current TRF turbine inlet condition corresponded to the minimum temperature measurement in the profile and although this profile was generated without coolant, the figure demonstrates how a relatively flat radial temperature profile can be misinterpreted as to having significant variation in the RTDF form.

Figure 3. The combustor exit temperature profiles re-plotted in the RTDF form.

After considerable review of the available combustor models and engine geometries presented in the current literature, five design criteria were selected for the new structure. The first requirement was installation into the true scale, fully annular, high pressure turbine rig located within the TRF at the AFRL. This first requirement dictated the size and scale of the device as well as the overall operating conditions. Secondly, an effective method for generating the representative pressure and temperature profiles was to design the simulator device such that it provided a means to inject several secondary flow streams, at varying flow rates, into one central annular chamber that contained an exit contraction. This second requirement resulted in the mainstream flow being divided into central and secondary flow paths. The third requirement was that the simulator device needed a means to thermally condition the secondary flow paths. This was accomplished by passively removing heat from the secondary flow streams using finned-tube heat exchangers. The simulator also needed a means to produce turbulence intensity levels that are typically present at the combustor exit between 10% and 20%, which was the fourth requirement. An effective method for producing high intensity, large scale turbulence is through the use of opposing jets in a cross-flow. This fourth requirement was met by incorporating multiple rows of opposing dilution jets that inject flow into the central chamber. The fifth requirement centered on the idea that the simulator needed refined control over the temperature and pressure profiles at radial locations near the turbine endwalls. This is accomplished through the use of

several rows of film cooling holes that inject flow over a range of flow rates.

Having established the five main design criteria, a more in-depth and thorough analysis was performed to determine the necessary pressure drops, flow splits, and heat transfer within the various flow paths. Before these analyses could begin a better understanding was needed of the facility into which the simulator was to be incorporated.

TURBINE RESEARCH FACILITY DESCRIPTION

The TRF is a turbine test facility located within the Turbine Engine Research Center at the AFRL at Wright-Patterson Air Force Base in Dayton, Ohio. The TRF, documented in Haldeman et al. [13], is a short duration blow-down test facility that is capable of matching several non-dimensional aerodynamic and thermal engine parameters. These parameters include Reynolds number, Mach number, pressure ratio, gas to metal temperature ratio, corrected speed, and corrected mass flow.

The facility, shown schematically in Figure 4, consists of a large supply tank, a turbine test section, and two large vacuum tanks. The test section is a true scale, fully annular, single turbine stage consisting of vanes and rotor blades. Prior to testing, nitrogen gas is pressurized and heated within the supply tank while the main turbine section and vacuum tanks are evacuated to near vacuum conditions. The turbine rotor is then driven by a starting motor to a speed slightly higher than the desired test speed. This motor is then turned off allowing the turbine rotor to decelerate to the test speed at which time an electrical eddy current brake is used to hold the rotor speed constant. Testing begins by activating the fast acting main valve that connects the supply tank to the main turbine test section. At this time, the gas flows from the supply tank through the turbine test section and into the vacuum tanks. The mass flow rate is set by controlling the turbine pressure ratio using a variable area isolation valve that is located downstream of the main test section. The duration of a typical test is between one and five seconds, depending on the size of the turbine that is being tested. Most of the above mentioned aero thermal parameters remain constant during testing including the pressure ratio, corrected speed, specific heat ratio, and local Mach number. But since the supply tank pressure and temperature both decay during the blow down, the test section Reynolds number, Prandtl number, and gas to metal temperature ratio vary during testing. These three parameters, however, are nearly steady over approximately twenty rotor revolutions and a steady state condition is assumed over these smaller time intervals.
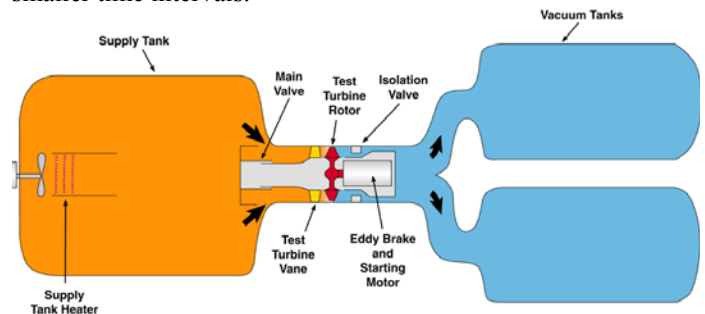

Figure 4. Schematic of the TRF facility.

Traverse rings are used to measure the turbine inlet and exit conditions. Each traverse ring contains multiple instrumentation rakes for mounting thermocouples and pressure transducers. The probes on each rake are spaced to obtain measurements over equal annular flow areas and during testing these rakes are traversed circumferentially approximately ninety degrees to obtain both radial and circumferential profiles. Due to the short test duration measurements are all recorded simultaneously in real time across 200 12-bit channels with a maximum frequency response of 100 kHz and 200 16-bit channels with a maximum frequency response of 200 kHz. Measurements are then time averaged over approximately twenty rotor revolutions.

OVERALL MECHANICAL DESIGN

The combustor simulator structure had to be designed to replace the turbine inlet section located downstream of the TRF supply tank and upstream of the main turbine test section. The existing inlet section, shown in Figure 5, consists of a primary flow annulus that directs the supply tank flow through a contraction, through the upstream traverse section, and into the turbine nozzle guide vanes. It also contains an inner flow annulus that is used to direct cooling flow to the turbine vanes and blades. This turbine inlet section was studied to determine the necessary upstream and downstream physical mating requirements so that the simulator could be installed.
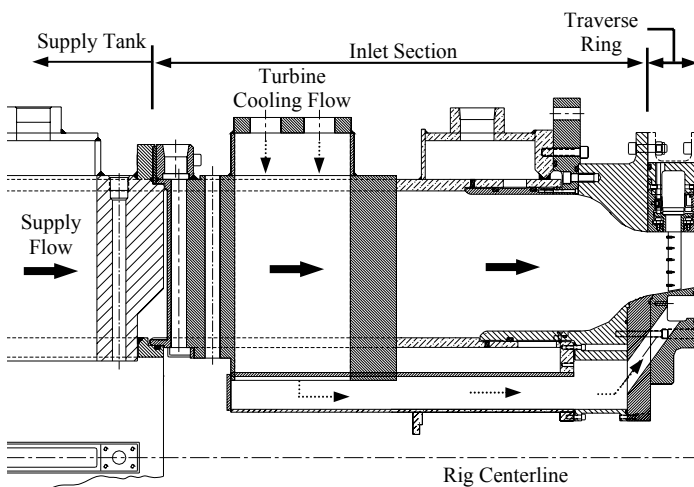

Figure 5. Drawing of the original TRF turbine inlet section.

The combustor simulator design divides the TRF supply tank flow into three concentric annular flow paths. The center annulus is further divided into three concentric annuli to direct a portion of the supply tank flow to the inlet of the central chamber and to the first of two rows of dilution holes. The inner and outer annular flow paths are used to thermally condition portions of the supply tank flow by directing the flow stream through finned-tube heat exchangers and then into the main central chamber through secondary dilution holes and film cooling holes that are located within the contraction section. The first row of opposing dilution jets acts as the primary turbulence generator by injecting flow at relatively large local momentum flux ratios. The first row dilution holes were designed to operate with a nominal momentum flux ratio,

I, near 100 which is consistent with an actual engine combustor. The second row dilution jets were designed to inject flow at much lower momentum flux ratios in the range of $I = 0$ to 25, also consistent with actual engine combustors, to help tailor the exit temperature profile. The film cooling holes were designed to shape both the exit temperature and pressure profiles by injecting flow over a range of momentum flux ratios between $I = 0$ to 20. A drawing showing the entire steel framework that was ultimately designed is shown in Figure 6.

The dilution holes were positioned axially on both the inner and outer diameter walls of the central chamber to be consistent with the spacing within actual combustors. The first row was placed at approximately $X / L = 0.45$ ($X / D_1 = 12.3$) and the second row was placed at approximately $X / L = 0.65$ ($X / D_2 = 11.6$) where L is the overall length of the central chamber. For the current tests, there are forty four holes in each row to match the forty four vanes. The first row is staggered with respect to the second row such that the center of a dilution hole in the second row is circumferentially in-line with the stagnation plane of the downstream vane. The center of a dilution hole in the first row is therefore circumferentially in-line with the vane mid-passage. The first row dilution holes each have a diameter of $D_1 = 1.27$ cm and the second row dilution holes each have a diameter of $D_2 = 1.91$ cm. These holes sizes were determined from a flow division and pressure drop analysis that is discussed in the next section and are consistent with dilution hole sizes in actual engine combustors. These hole sizes and numbers resulted in a pitchwise spacing of $Y / D_1 = 2.6$ and $Y / D_2 = 1.8$ for the inner diameter side of the central chamber and $Y / D_1 = 4.3$ and $Y / D_2 = 2.9$ for the outer diameter side. The ability to circumferentially rotate the second row of dilution holes with respect to the first row was incorporated into the structural design of the simulator. This allows the possibility to study the effects of dilution hole alignment on profile generation and how this affects the flow development and heat transfer within the turbine.
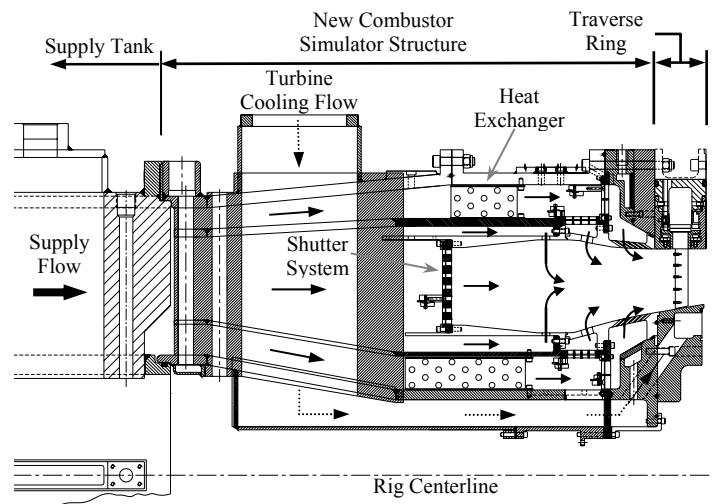

Figure 6. Drawing showing the new combustor simulator framework within the TRF.

The inner and outer diameter contraction rings of the main central chamber each contain six rows of staggered film cooling holes each having a diameter of $D_{FC} = 0.32$ cm. The film

cooling hole diameter was chosen such that the ratio of axial distance to hole diameter between the last row of holes and the turbine vane inlet was consistent with actual engine values. They were arranged in a multiple row staggered pattern resulting in a streamwise spacing of $X / D_{FC} = 3.0$ and an average pitch spacing of $Y / D_{FC} = 3.6$ for the inner diameter contraction ring and an average pitch spacing of $Y / D_{FC} = 3.4$ for the outer diameter contraction ring. These spacing parameters are shown in Figure 7. The ratio of total film cooling hole area to combustor exit flow area is approximately 0.033 for the inner diameter and 0.052 for the outer diameter. It is important to note that this streamwise spacing is different from most film cooling hole applications where the purpose is to provide an effective cooling layer of the hardware surface. The film cooling holes in the current application, however, are used to specifically help create a broad range of exit pressure and temperature profiles.
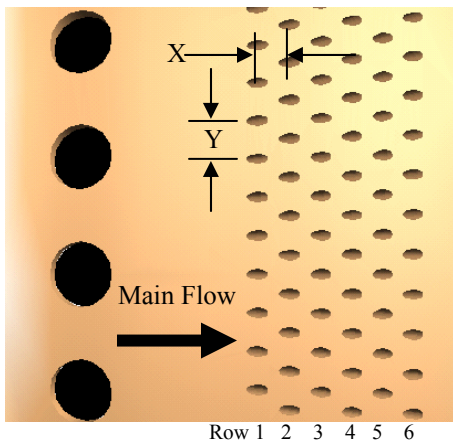

Figure 7.   Drawing highlighting the hole spacing parameters for the inner diameter contraction ring.

The contraction rings containing the dilution and film cooling holes were not only designed to be capable of circumferential rotation but they were also designed to be replaceable. First, it allows the simulator to be tested with different turbines that have their inlet nozzle guide vanes at different radial locations. Secondly, it allows different film cooling hole patterns to potentially be studied in the future. This could include holes that inject the film cooling flow circumferentially as well as axially to study influences of near wall swirl. The effects of the contraction rings with more holes, less holes, smaller holes, bigger holes, or even no holes at all could be studied.

FLOW DISTRIBUTION AND CONTROL

In addition to sizing the annular flow paths, direct flow control is accomplished through the use of five adjustable shutter systems. Each system consists of one rotating disc and one non-rotating disc that both contain the exact same hole pattern. By positioning the rotating disc with respect to the non-rotating disc the blockage in a particular flow stream can be increased or decreased. This controllable flow blockage, or solidity ratio, acts as an adjustable pressure drop thus allowing the flow in a particular path to be controlled. The solidity ratio, β, is defined to be one minus the ratio of the total open flow area to the total annular flow path area. The solidity ratio has a

range between zero and one where zero corresponds to a fully open annulus and one corresponds to a fully closed annulus. The five shutters are located at the inlet of the main central chamber, the inlets of the second row dilution plenums in both the inner and outer secondary flow paths, and the inlets of the film cooling plenums in both the inner and outer secondary flow paths as shown in Figure 6.

The design of each shutter system involved performing a study to determine the most effective hole pattern and shape. Ultimately, it was found that circumferential slots met the optimal design goals much better than circular holes for all of the patterns that were considered. The circumferential slots are limited by the inner and outer diameter edges of the shutter discs, however, they are not limited in the circumferential direction and could span any angle that was chosen. However, due to concern over non-uniform flow exiting the shutters around the entire annulus, this circumferential angle for each slot was limited to near 15° to ensure multiple slots existed in each row per 90° of the annulus.

The optimal design for the shutter systems located within the two secondary flow paths was one that exhibited a behavior such that the range of annular flow path solidity was large while minimizing the sensitivity to changes in the shutter rotation angle. This behavior is illustrated in Figure 8 where it can be seen that the relationship between shutter rotation angle and annular flow path solidity ratio is linear for the circumferential slots. In addition, it was also important for the shutter designs to have a uniform as possible exit flow to minimize unwanted circumferential discontinuities. This additional design requirement resulted in the shutter designs with staggered slot patterns being the most desirable. The shutter system located at the inlet of the central chamber required a different type of design. Its optimal design is one that exhibits a behavior such that a large range of shutter rotation angle results in a small range of annular flow path solidity ratio. This is because the solidity of this shutter will always remain near the fully closed position for all flow conditions and small changes in β here will result in drastic changes to the overall flow splits.
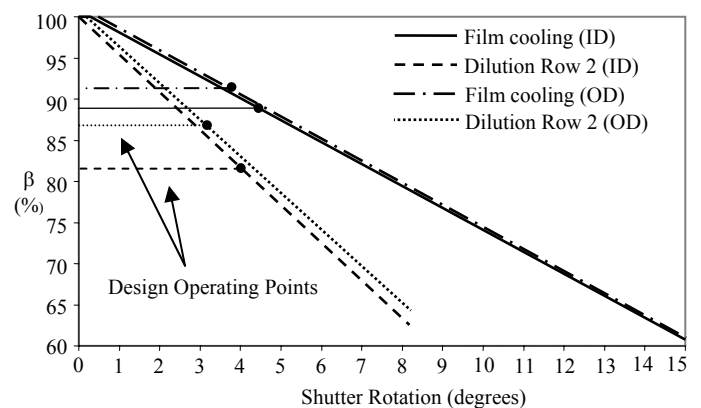

Figure 8.   Plot showing the design behavior of the shutter systems in the secondary flow paths.

Since the flow control shutter systems were the obvious weakest structural link in the entire simulator framework, a force and stress analysis of these devices was performed via the Components Branch at the AFRL. The individual part

drawings were imported into ANSYS to test the strength of the shutter components when exposed to typical blow down pressures and temperatures, nominally 450 kPa at 480 K. The results from these analyses helped to identify regions with high stress concentrations so that parts could be redesigned if necessary. These high stress concentrations were typically found surrounding bolt holes and in locations between adjacent circumferential slots. None of the shutters experienced overall stress levels above the yield point of the steel part, however, to ensure a high factor of safety some design features were modified. A vibration analysis of the shutter systems was not performed since it is expected that during testing each rotating component will be pressed firmly downstream against its non-rotating counterpart thereby resulting in minimal vibration. In addition, each shutter system delivers its flow into a small plenum annulus before it is injected into the central chamber mainstream. These plenum cavities provide a flow mixing and diffusion region to help eliminate any flow circumferential non-uniformities or vibration pulses created due to the shutters.

The motion control systems that were designed to control the rotation of each shutter consisted primarily of a rack and pinion system driven by a highly resolved stepper motor. Figure 9 shows the design concept. The motors were each equipped with a 2000 pulse per revolution encoder that can control the motor shaft rotation to within 0.18° and shutter rotation to within 0.05°. The controller and motor lead wires are directly connected to an Anahiem Automation SMC40 Single Axis Indexer. Hermetically sealed, high temperature rated limit switches were purchased from Haydon Switch and Instrument and two will be incorporated into each shutter system. The switches will be fastened to a non-rotating wall such that when the shutter rack rotates to a certain position it will engage the switch and activate an electrical signal to identify either a *home* or *end-of-travel* position. The *home* position will correspond to a fully closed shutter and will be used as a starting point for each test.
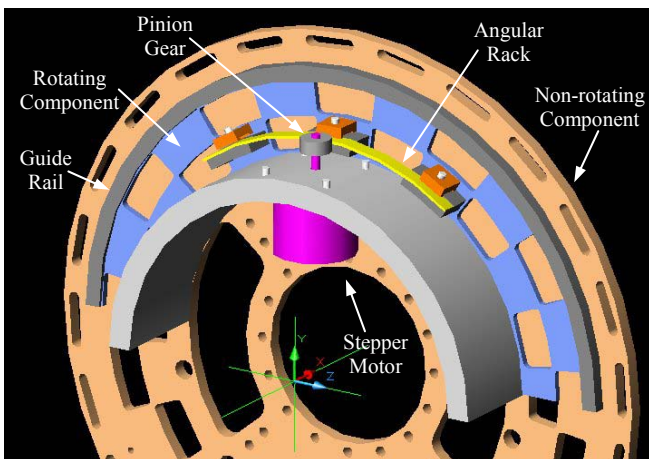

Figure 9. Drawing showing the drive system concept for the shutter systems.

The operating points of the shutter systems for the various combustor profiles were determined by performing a one-dimensional flow division and pressure drop analysis using a computational code that was written in Matlab. The flow temperature, pressure, and mass flow rate are all calculated at several locations within the simulator device based on the given supply tank conditions. For each flow path, the pressure drop is calculated as the flow progresses from one location to the next beginning within the supply tank and ending inside the central chamber. The design and analysis goal was to establish a pressure drop system, via the shutters, that resulted in the first row dilution holes experiencing their design momentum flux ratio ($I = 100$) while at the same time resulting in the second row dilution holes and film cooling holes experiencing momentum flux ratios in the middle of their operating ranges. The most significant pressure drop calculations include those occurring across the shutter systems, across the heat exchangers, and across the walls defining the central chamber.

THERMAL MANAGEMENT

The best way to achieve a broad range of combustor exit temperature profiles was to only thermally condition the flow passing through the two secondary flow paths. This decision meant that the central annulus, which contains the majority of the mass flow, would deliver flow to the central chamber inlet and first row dilution holes at the elevated supply tank temperature. This is in contrast to the Virginia Tech simulator, documented in Barringer et al. [3], that contains two rows of dilution holes that both inject flow at the cooled secondary flow temperature. The overall goal in this decision was to maintain the mass-averaged flow temperature at the combustor simulator exit at an elevated level with respect to the secondary flow path temperatures. This elevated exit temperature scenario is desirable to ensure large operational temperature differences for better measurement resolution.

Incorporating two rows of dilution holes that can inject flow into the central chamber at different temperatures has another important design advantage. Since the dilution hole rows are staggered and spaced in the circumferential direction to match the pitch spacing of the vanes, circumferential hot spots will be generated that alternate from hot to cold at the combustor exit that also match the pitch spacing of the vanes. This will help create a more realistic exit temperature profile that varies in both the circumferential and radial directions. Plans for the facility also include investigating non-symmetric circumferential hot spots by plugging certain second row dilution holes thereby limiting the amount of dilution coolant injected into a localized circumferential region, but this has not yet been implemented.

The type of heat exchangers that were designed consisted of stainless steel axial fins and circumferential tubes. Each heat exchanger was divided into two 180° sections with supply and return manifolds placed at both ends. The manifolds are used to evenly disperse the tube side fluid flow through the various tubes. This tube side flow will be circulated prior to testing to establish the desired initial metal temperature in each unit. Dividing each unit into two identical sections was done to combat any vertical thermal stratification present in the simulator due to natural convection. Different amounts of fluid flow can be sent through the upper half of the annulus versus the lower half of the annulus to achieve the desired operating temperatures.

To determine the transient annulus flow temperature exiting the heat exchanger it was necessary to first determine the heat exchanger metal temperature as a function of time during testing. The metal temperature was investigated using a thermodynamic analysis on a control volume surrounding the

heat exchanger. The convection heat transfer coefficient for the annulus gas passing through each unit, h_{gas}, was approximated using published data in Kays and London [14] from a performance curve given for a finned-tube heat exchanger geometry similar to the one that was designed. The data is in the form of a relationship between the Colburn factor, j, and the Reynolds number, Re_G, and was approximated using the function $j = 0.1696Re_G^{-0.4014}$.

Knowing the annulus mass flow rate in time, the heat exchanger geometry, and the gas inlet temperature to the heat exchanger in time, the value of Re_G was determined as a function of time. This then allowed the determination of the Colburn factor and finally the heat transfer coefficient as a function of time. The in depth, transient analysis model included lengthy differential equations that were coded into Matlab and a fourth-order Runge-Kutta numerical integration scheme was written to solve for the heat exchanger metal temperature as a function of time. Once the metal temperature had been determined, the annulus flow temperature exiting the heat exchanger could be determined as a function of time.

A simple lumped capacitance (SLC) model was also included in the overall analysis to compare the predicted results of the more in depth model to make sure they were reasonable. This SLC model is the standard one-dimensional transient model governed by equation 1.

$$\frac{T_{metal}(t) - T_{gas}}{T_{metal_i} - T_{gas}} = \exp\left(\frac{h_{gas} \cdot A_{metal} \cdot t}{\rho_{metal} \cdot c_{p_{metal}} \cdot Vol_{metal}}\right) \qquad (1)$$

This equation is only applicable, however, for no tube fluid flow and when the gas temperature at the inlet of the heat exchanger and h_{gas} are constant in time. Nevertheless, it was decided to still use the equation on a comparative basis. Figure 10 shows computational results for both models when the inner diameter heat exchanger is exposed to typical blow down conditions with an initial metal temperature equal to the initial supply tank temperature.
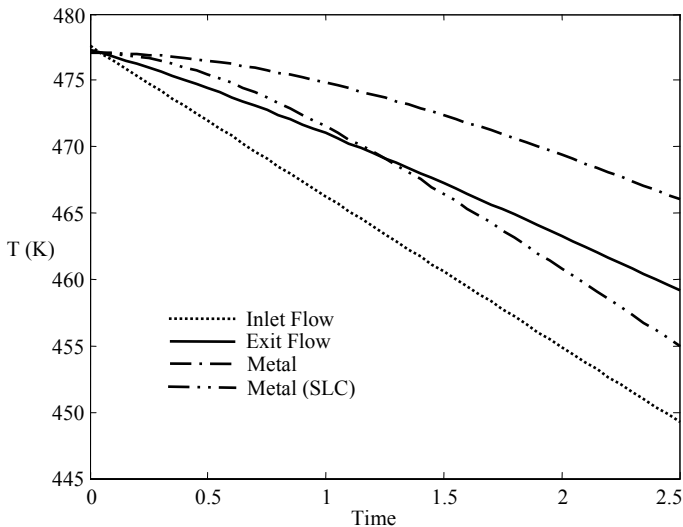
Figure 10. Predicted exit flow temperature for the inner annulus heat exchanger for an initial metal temperature that equals the initial supply tank temperature.

The response of the inner diameter heat exchanger units to the design annulus mass flow conditions can be seen in Figure 11 when using an initial metal temperature near room temperature. It can be seen that the initial temperature drop predicted is near 75 K. This temperature drop, however, decreases as the test time progresses to values near 40 K. This reduction in temperature drop is explained by the fact that the relatively cold metal quickly heats up as the hot supply tank gas passes through the heat exchanger. The behavior of the exit flow temperature was considered optimal from a test standpoint since a reasonable temperature drop was produced and the exit gas flow temperature remained nearly constant during the test.
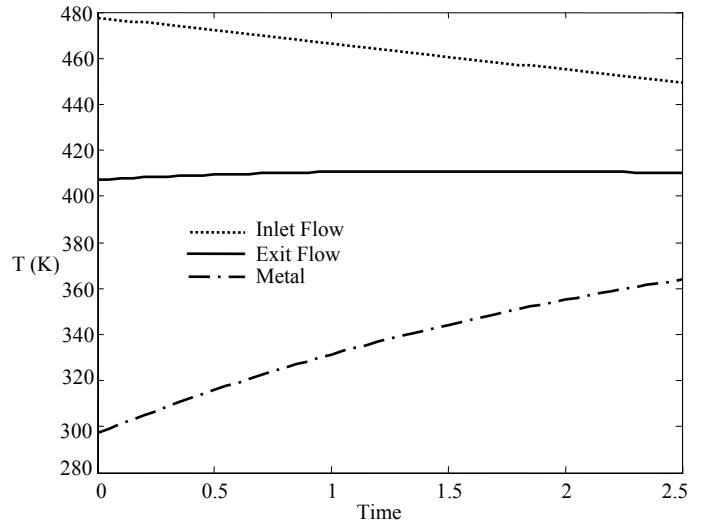
Figure 11. Plot showing the thermal response of the inner diameter heat exchanger design using an initial metal temperature near room temperature.

Additional thermal management comes in the form of maintaining certain metal wall temperatures prior to testing including the vanes and rotor to establish the correct T_{gas} / T_{metal}. This is accomplished by utilizing a series of water cooling jackets. These cooling jackets are strategically placed at axial locations corresponding to the interface between the supply tank main valve and the combustor simulator inlet as well as the interface between the combustor simulator exit and the traverse section inlet. The water cooling jackets also required a delivery system to be designed.

COMBUSTOR SIMULATOR INSTRUMENTATION
Several types of measurements are needed to benchmark the overall performance of the simulator. These include measurements of total pressure, static pressure, velocity, flow temperature, and surface temperature. An instrumentation plan was developed to locate the places within the simulator to perform these measurements. Figure 12 shows a schematic of the simulator highlighting these positions and their corresponding measurement.

Total pressure measurements will be made to quantify the pressure drops across the flow control shutters, heat exchangers, and central chamber walls. These measurements will be made using several in-house Kiel pressure probes. Total pressure measurements will also be made within the plenum chambers of the second row dilution holes and film cooling holes. Kiel pressure probes will also be positioned at

the exit of several dilution holes to help verify the amount flow passing through each dilution row. Static pressure measurements will be made on the surface of the inner and outer diameter contraction rings at an axial location upstream of the film cooling holes to help determine the amount of flow exiting the film cooling holes. These measurements will be made using high temperature, miniature Kulite pressure transducers. Velocity measurements will be made using several custom pitot static pressure probes placed upstream and downstream of each heat exchanger as well as the center annulus main shutter.
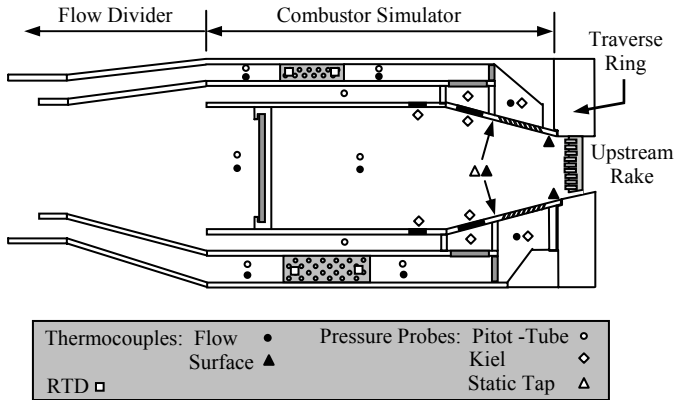

Figure 12. Schematic of the combustor simulator highlighting the instrumentation plan.

Temperature measurements will be made using thermocouples and resistance temperature detectors (RTD). The flow temperature at various locations within the simulator will be made using in-house thermocouple probes. Each probe is made using Omega type E thermocouple wire and contains approximately a 0.0127 cm diameter bead. These thermocouple probes will be used to monitor the flow temperature upstream and downstream of the heat exchangers. Surface temperature measurements will be made using Omega RTDs to monitor the heat exchanger metal temperatures before and during testing. Omega cement-on thermocouples will be used to monitor the metal temperatures of the inner and outer diameter contraction pieces both upstream and downstream of the film cooling holes.

BENCHMARK TESTS

Once the combustor simulator is assembled and instrumented it will be installed into the TRF rig for testing. Before studying the effects of the various exit profiles on turbine vane heat transfer, aerodynamic loading, and secondary flow development, a series of benchmark tests will be needed to determine the overall performance of the simulator device. These initial tests were determined by performing a Taguchi analysis, documented in Kacker and Tsui [15], to minimize the number of initial test runs needed. A total of nine input factors were selected including the initial supply tank temperature and pressure, the initial metal temperatures of the two heat exchangers, and the annular solidity ratios of the five adjustable shutters. Each of these input factors has an upper and lower limit, shown in Table 1, that was determined based on the component operating limits.

Table 1. Nine Input Factors with Ranges

Input Factors	Lower Level	Upper Level
(1) Supply Tank Pressure (kPa) - Initial	210	550
(2) Supply Tank Temperature (K) - Initial	365	480
(3) ID Heat Exchanger T_{metal} (K) - Initial	295	480
(4) OD Heat Exchanger T_{metal} (K) - Initial	295	480
(5) Central Chamber Shutter β (%)	85	95
(6) ID Film cooling Shutter β (%)	65	95
(7) OD Film cooling Shutter β (%)	65	95
(8) ID 2nd Row Dilution Shutter β (%)	65	95
(9) OD 2nd Row Dilution Shutter β (%)	65	95

The system outputs are the pressure and temperature profiles at the combustor simulator exit, and therefore consist of one set of nine pressure probes and one set of nine thermocouple probes that are mounted on two separate instrumentation rakes. These probes will be traversed approximately ninety degrees in the circumferential direction during testing to determine both radial and circumferential variations in pressure and temperature. These first tests will provide a large data set that will include sixteen different combustor exit temperature and pressure profiles.

The knowledge gained from these initial tests will be used to determine the input factor settings needed to tweak the exit profiles at certain radial locations. The affects of these various temperature and pressure profiles on turbine vane aerodynamic loading, secondary flow development, and surface heat transfer will ultimately be studied. These tests will require several miniature pressure transducers to be mounted along both the pressure and suction surfaces of a vane at 50% and 96.5% span similar to the instrumented TRF blade shown in Figure 13. The nine-headed probe rakes will be positioned upstream *and* downstream of the turbine vane passage to measure radial and circumferential pressure and temperature.
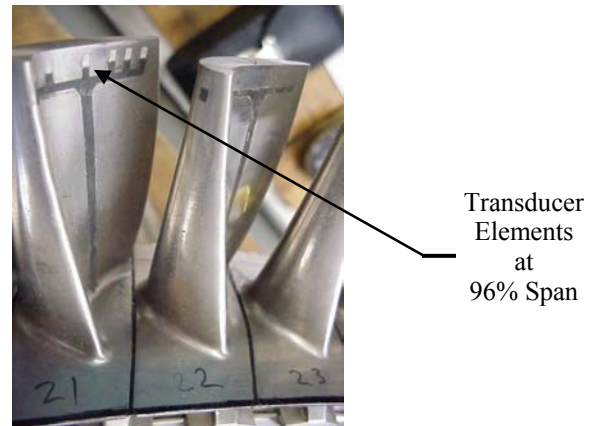

Figure 13. TRF turbine blade instrumented with miniature Kulite pressure transducers.

Oxford style thin film heat flux gauges, documented in Piccini et al. [16], will be installed on the surface of three vanes at span locations of 24%, 60%, and 96%, similar to that shown in Figure 14, as well as on the endwalls. Augmentation levels of heat flux, vane pressure distribution, and airfoil wake pressure distribution will be reported based on a flow profile

9   Copyright © 2004 by ASME

case with a relatively constant radial pressure and temperature exiting the simulator. Experiments may also be performed to study the effect of changing the circumferential position of the second row dilution holes such that they are in-line with the first row and how this alignment affects the combustor exit profiles.
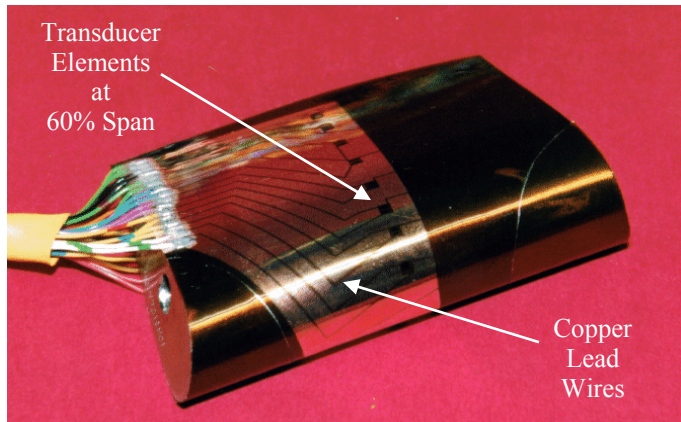

Figure 14. TRF turbine vane instrumented with an Oxford thin film heat flux gauge.

Turbulence intensity and length scale will be investigated using two TSI hotwire probes and a thermal anemometry system. The probes will be mounted in the same traverse system as the pressure probe rakes located downstream of the simulator and upstream of the turbine vanes. A thermocouple will be installed on the probe to allow the temperature of the flow to be determined in close proximity to the hotwire sensor element. Due to the transient nature of the test rig and the varying elevated flow temperatures, hotwire measurements will have to be conducted under separate isothermal test conditions where all flow streams are approximately at the same temperature. It will also require an in-situ blowdown calibration of the hotwire using the procedure documented in Holmberg [17] and Nix et al. [18] and a pitot static pressure probe located in close proximity to the hotwire probe. Increases or decreases in turbulence intensity and length scales exiting the simulator will also be documented relative to the baseline flow case. The turbulent lengths scales should scale well with the dilution hole diameters.

Contour maps of temperature at the inlet of several vane passages will be made to fully document the non-uniform thermal loading. The thermocouple rakes located upstream and downstream of the vane passage will be used to study hot spot migration through the vane passage. The downstream temperature measurements will also be used to document how the upstream film cooling flow migrates through the vane passage near the endwall.

CONCLUSIONS

It is believed that the combustor simulator structure that was designed in this work will provide the means necessary to produce a variety of turbine inlet profiles that are representative of actual engine conditions with realistic turbulence intensity levels. The significance of performing this research resides in its potential contribution to improving turbine engine hardware as well as educating researchers and engine designers of the effects of different turbine inlet profiles.

Understanding how the flow and thermal fields exiting aircraft engine combustors interact with the turbine nozzle guide vanes, endwall regions, and blades will allow significant improvements to be made in component design and working life. The complex temperature and pressure profiles exiting combustors have forced engine designers to prepare for the worst case without knowing exactly how the profiles affect the hardware. In addition, by incorporating the means to control the turbine inlet profile it is hoped that the unsteadiness on the vanes and blades will be affected by reducing secondary flows. This would ultimately serve to reduce vibration and high cycle fatigue issues on the turbine.

ACKNOWLEDGMENTS

REFERENCES

[1] Holdeman, J.D., 1993, "Mixing of Multiple Jets with a Confined Subsonic Crossflow," *Prog. Energy Combust. Sci.*, Vol. 19, pp. 31-70.

[2] Ames, F.E. and Moffat, R.J., 1990, "Effects of Simulated Combustor Turbulence on Boundary Layer Heat Transfer," Heat Transfer in Turbulent Flow 1990: AIAA/ASME Thermophysics and Heat Transfer Conference, Seattle, Washington, June 18-20, 1990.

[3] Barringer, M., Richard, O., Stitzel, S., Walter, J., and Thole, K., 2002, "Flow Field Simulations of a Gas Turbine Combustor," *Journal of Turbomachinery*, Vol. 124, pp. 508-516

[4] Stitzel, S. and Thole, K. A., 2003, "Flow Field Computations of Combustor-Turbine Interactions Relevant to a Gas Turbine Engine," ASME Paper GT-2003-38253.

[5] Cameron, C., Brouwer, J., Wood, C., and Samuelsen, G., 1989, "A Detailed Characterization of the Velocity and Thermal Fields in a Model Can Combustor with Wall Jet Injection," *Journal of Engineering for Gas Turbines and Power*, Vol. 111, pp. 31-35.

[6] Bicen, A., Tse, D., and Whitelaw, J., 1988, "Flow and Combustion Characteristics of an Annular Combustor," *Combustion and Flame*, Vol. 72, pp. 175-192.

[7] Schwab, J., Stabe, R. and Whitney, W., 1983, "Analytical and Experimental Study of Flow Through an Axial Turbine Stage With a Nonuniform Inlet Radial Temperature Profile," AIAA 83-1175.

[8] Stabe, R., Whitney, W., and Moffit, T., 1984, "Performance of High-Work Low-Aspect Ratio Turbine Tested with a Realistic Inlet Radial Temperature Profile," AIAA 84-1161.

[9] Chana, K., Hurrion, J., Jones, T., 2003, "The Design, Development and Testing of a Non-Uniform Inlet Temperature Generator for the QinetiQ Transient Turbine Research Facility," ASME 2003-GT-38469.

[10] Krishnamoorthy, V., Pai, B., and Sukhatme, S., 1988, "Influence of Upstream Flow Conditions on the Heat Transfer to Nozzle Guide Vanes," *Journal of Turbomachinery*, Vol. 110, pp. 412-416.

[11] Colban, W.F., Thole, K.A., and Zess, G., 2002, "Combustor Turbine Interface Studies – Part 1: Endwall Effectiveness Measurements," ASME 2002-GT-30526.

[12] Hermanson, K. and Thole, K., 2000, "Effect of Inlet Conditions on Endwall Secondary Flows," AIAA 99-0241.

[13] Haldeman, C.W., Dunn, M.G., MacArthur, C.D., and Murawski, C.G., 1992, "The USAF Advanced Turbine Aerothermal Research Rig (ATARR)," NATO AGARD Propulsion and Energetics Panel Conference Proceedings 527, Antalya, Turkey.

[14] Kays, W.M. and London, A.L., 1964, Compact Heat Exchangers. New York: McGraw-Hill Inc.

[15] Kacker, R. and Tsui, K., 1990, "Interaction Graphs: Graphical Aids for Planning Experiments", *Journal of Quality Technology*, Vol. 22, No. 1.

[16] Piccini, E., Guo, S., and Jones, T., 2000, "The Development of a New Direct-Heat-Flux Gauge for Heat-Transfer Facilities," *Measurement Science Technology*, Vol. 11, pp. 342-349.

[17] Holmberg, D.G., 1996, "A Frequency Domain Analysis of Surface Heat Transfer/Freestream Turbulence Interactions in a Transonic Turbine Cascade," PhD. Dissertation, Virginia Tech.

[18] Nix, A., Smith, A., Diller T., Ng, W., and Thole, K., 2002, "High Intensity, Large Length-Scale Freestream Turbulence Generation in a Transonic Turbine Cascade" ASME paper GT-2003-30523.